doi:10.1038/nature09171

LETTERS

Regulation of myeloid leukaemia by the cell-fate determinant Musashi

Takahiro Ito[1]*, Hyog Young Kwon[1]*, Bryan Zimdahl[1], Kendra L. Congdon[1], Jordan Blum[1], William E. Lento[1], Chen Zhao[1], Anand Lagoo[2], Gareth Gerrard[3], Letizia Foroni[3], John Goldman[3], Harriet Goh[4], Soo-Hyun Kim[4], Dong-Wook Kim[4], Charles Chuah[5], Vivian G. Oehler[6], Jerald P. Radich[6], Craig T. Jordan[7] & Tannishtha Reya[1]

Chronic myelogenous leukaemia (CML) can progress from a slow growing chronic phase to an aggressive blast crisis phase[1], but the molecular basis of this transition remains poorly understood. Here we have used mouse models of CML[2,3] to show that disease progression is regulated by the Musashi–Numb signalling axis[4,5]. Specifically, we find that the chronic phase is marked by high levels of Numb expression whereas the blast crisis phase has low levels of Numb expression, and that ectopic expression of Numb promotes differentiation and impairs advanced-phase disease *in vivo*. As a possible explanation for the decreased levels of Numb in the blast crisis phase, we show that NUP98–HOXA9, an oncogene associated with blast crisis CML[6,7], can trigger expression of the RNA-binding protein Musashi2 (Msi2), which in turn represses Numb. Notably, loss of Msi2 restores Numb expression and significantly impairs the development and propagation of blast crisis CML *in vitro* and *in vivo*. Finally we show that Msi2 expression is not only highly upregulated during human CML progression but is also an early indicator of poorer prognosis. These data show that the Musashi–Numb pathway can control the differentiation of CML cells, and raise the possibility that targeting this pathway may provide a new strategy for the therapy of aggressive leukaemias.

Chronic myelogenous leukaemia (CML) is initiated by the BCR–ABL translocation, which leads to myeloid cell expansion while allowing differentiation[8–11]. Secondary translocations such as NUP98–HOXA9 or AML1–EVI1, or mutations in p53 or INK4A/ARF, trigger progression through an accelerated phase to a blast crisis phase, with progressive loss of the capacity to differentiate[1]. Although blast crisis CML is, in part, more aggressive because of arrested differentiation, the pathways that underlie this arrest remain poorly understood. To determine whether CML progression may be driven by reversal of signals that regulate differentiation during normal development, we focused on Numb[4], a molecule that can be inherited differentially during asymmetric division and specify a committed fate[12–16].

To determine whether Numb regulates leukaemia progression we used mouse models representing chronic phase and myeloid blast crisis CML. Chronic disease was generated by infecting haematopoietic stem-cell-enriched populations (c-Kit$^+$Lin$^-$Sca-1$^+$ or KLS) with BCR–ABL and transplanting them into irradiated recipient mice[2,3]. Myeloid blast crisis was modelled by transplanting KLS cells transduced with BCR–ABL and NUP98–HOXA9 (refs 6, 7, 17). Using these we found that Numb was expressed at significantly lower levels in the blast crisis phase compared with the chronic phase (Fig. 1a–c). The decreased expression of Numb in the blast crisis phase indicated that keeping Numb at low levels may be essential for maintaining an immature state and that increasing its levels could trigger differentiation and inhibit disease progression. To test this possibility, haematopoietic cells were infected with BCR–ABL and NUP98–HOXA9 together with either control vector or Numb, transplanted and leukaemia progression monitored. A total of 83% of control mice developed leukaemia compared with 63% of those transplanted with Numb-expressing cells (Fig. 1d). Notably, leukaemias that developed in the presence of Numb were more differentiated (Fig. 1e, f) and unable to propagate disease efficiently (93% versus 20%, Fig. 1g) or infiltrate secondary organs (Fig. 1h, i and Supplementary Fig. 1); no signs of leukaemia were detected in mice that survived (Fig. 1j and Supplementary Fig. 1). Numb also impaired propagation of fully established leukaemias and markedly reduced the frequency of cancer stem cells (Supplementary Fig. 2). These data show that continual repression of Numb is essential for maintenance of blast crisis CML, and that increasing the levels of Numb can inhibit disease.

Because Numb can antagonize Notch signalling in several systems[13,18,19], we tested whether Numb and Notch had a reciprocal relationship in CML. Notch signalling was elevated in blast crisis CML (Supplementary Fig. 3), and its inhibition via dominant negative *Xenopus* Suppressor of Hairless (dnXSu(H)) delivery or through conditional deletion of Rbpj paralleled the effects of Numb and led to reduced incidence and propagation of blast crisis CML (Supplementary Fig. 4). Furthermore, levels of p53, another Numb target[20], were higher in Numb-expressing blast crisis CML (Supplementary Fig. 5a). In the absence of p53, Numb was unable to affect leukaemic cell growth *in vivo* or *in vitro* (Supplementary Fig. 5b–f), indicating that Numb's effects are in part dependent on p53.

The observation that Numb repression was critical for the maintenance of blast crisis CML led us to seek the mechanism by which Numb may be downregulated in this context. We focused on the RNA-binding protein Musashi (Msi), which has been shown in the nervous system to repress Numb by binding the 3′ untranslated region (UTR) of the transcript[21]. Msi was originally identified in *Drosophila* as a regulator of asymmetric division[5,22] and its expression has been associated with stem and progenitor cells in several tissues[23,24]. In the haematopoietic system we found that Msi2 was expressed at much higher levels than Msi1 (Fig. 2a), and was particularly elevated in stem cells (Fig. 2b). Paralleling this, Msi2 expression was tenfold higher in the more immature blast crisis CML (Fig. 2c); this pattern held true even in matched lineage-negative fractions (Fig. 2d), indicating that Msi2 upregulation in the advanced phase

[1]Department of Pharmacology and Cancer Biology, Duke University Medical Center, Durham, North Carolina 27710, USA. [2]Department of Pathology, Duke University Medical Center, Durham, North Carolina 27710, USA. [3]Department of Haematology, Imperial College London, Hammersmith Hospital, London W12 0NN, UK. [4]Division of Hematology, Seoul St Mary's Hospital, The Catholic University of Korea, Seoul, Korea. [5]Department of Haematology, Singapore General Hospital, Cancer and Stem Cell Biology Program, Duke-NUS Graduate Medical School, Singapore. [6]Clinical Research Division, Fred Hutchinson Cancer Research Center, Seattle, Washington 98109, USA. [7]James P. Wilmot Cancer Center, University of Rochester School of Medicine, Rochester, New York 14642, USA.
*These authors contributed equally to this work.

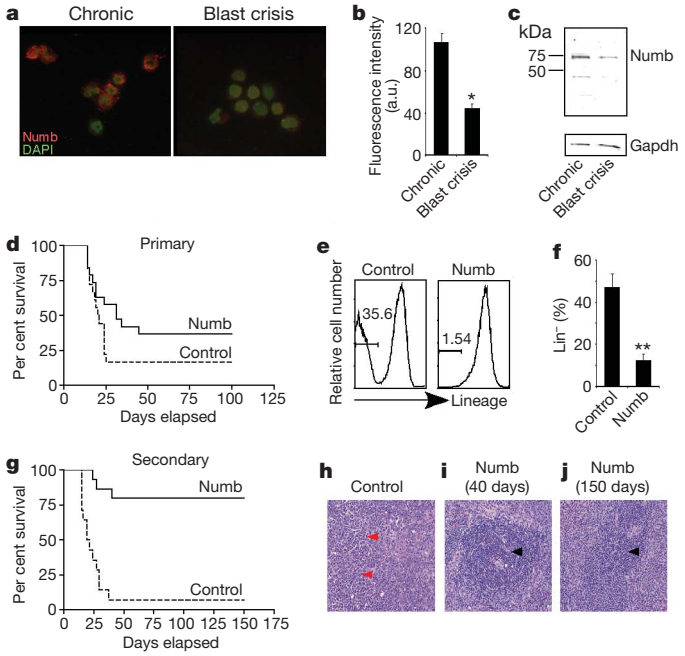

Figure 1 | Expression of Numb impairs blast crisis CML development. **a**, **b**, CML cells were immunostained with anti-Numb antibody (red) and 4′,6-diamidino-2-phenylindole (DAPI, green pseudocolour) (**a**), and fluorescence intensity was quantified, $*P < 0.05$ (**b**). a.u., arbitrary units. **c**, CML cells were analysed by western blot for Numb expression. **d**, Cells infected with BCR–ABL, NUP98–HOXA9 and either control vector or Numb were transplanted and survival was monitored (control, $n = 18$; Numb, $n = 19$). **e**, **f**, Representative (**e**) and average frequency of Lin^- cells (**f**) from control or Numb expressing leukaemias. $**P < 0.001$. **g**, Donor-derived cells from primary leukaemias were serially transplanted and survival monitored (vector, $n = 14$; Numb, $n = 15$; $**P < 0.001$). **h**–**j**, Haematoxylin-and-eosin-stained spleen sections from control vector (**h**) or Numb expressing leukaemias (**i**) or surviving mice (**j**). Immature myeloid cells (red arrowheads) and lymphoid follicles (black arrowheads) are indicated. Original magnification, ×10. Error bars in all bar graphs are s.e.m. Data shown are representative of three to four independent experiments.

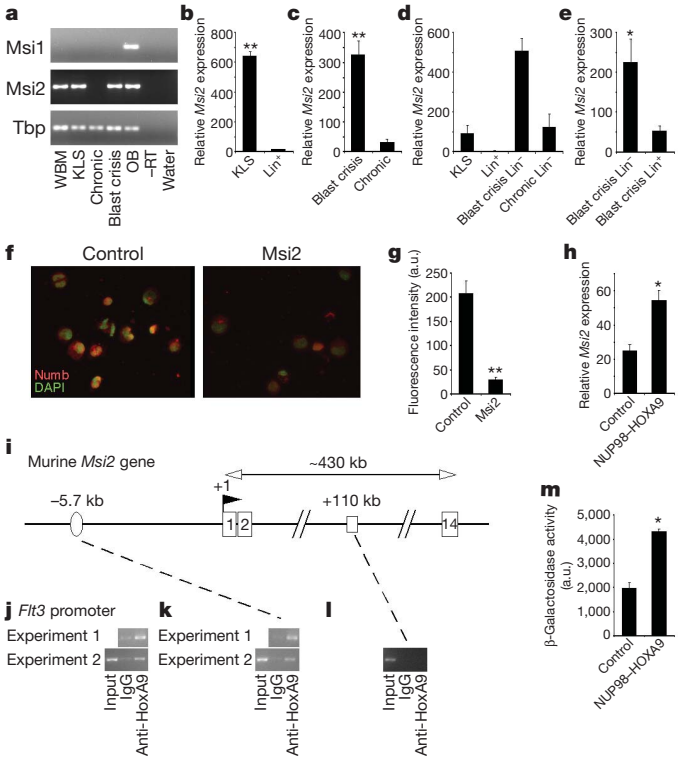

Figure 2 | The RNA-binding protein Musashi is highly expressed in immature normal and leukaemic cells and is regulated by HoxA9. **a**, Musashi (Msi) expression in whole bone marrow (WBM), KLS cells, chronic and blast crisis CML, olfactory bulb (OB), −reverse transcriptase (−RT in OB) and water. Tbp, TATA-binding protein. **b**–**e**, Real-time RT–PCR analysis of *Msi2* expression in KLS cells ($n = 3$) and Lin^+ cells ($n = 2$) (**b**), blast crisis phase ($n = 9$) and chronic phase ($n = 6$) (**c**), Lin^- chronic and blast crisis phase cells relative to normal KLS and Lin^+ cells (Lin^+, $n = 2$ and others, $n = 3$) (**d**), and Lin^- ($n = 5$) or Lin^+ ($n = 5$) blast crisis CML cells (**e**). Error bars represent s.e.m.; $*P = 0.039$; $**P < 0.001$. **f**, **g**, Control vector- or Msi2-expressing CML cells were stained with anti-Numb antibody (red) and DAPI (green pseudocolour) (**f**), and fluorescence intensity was quantified (**g**). $**P < 0.001$. **h**, Msi2 expression in KLS cells transduced with either control vector or NUP98–HOXA9 retrovirus along with BCR–ABL. $*P = 0.017$. **i**–**l**, HoxA9 binds to the *Msi2* promoter. Murine *Msi2* gene structure: numbered boxes indicate exons; transcription start site (TSS) and the direction of transcription are indicated by +1 and the black flag, respectively; the oval indicates putative HOX binding element 5.7 kb upstream of TSS; the open rectangle indicates +110 kb site with no HoxA9 binding sequence. ChIP was performed either with IgG control or anti-HoxA9 antibody for *Flt3*, a known HoxA9 target gene, as a positive control (**j**), and for *Msi2* −5.7 kb region (**k**) or *Msi2* +110 kb region (**l**). **m**, KLS cells from Msi2 gene-trap reporter mice were transduced with BCR–ABL and either control vector or NUP98–HOXA9, and β-galactosidase reporter activity was quantified ($n = 2$ each; $*P = 0.011$). a.u., arbitrary units.

is not simply a consequence of altered cellular composition. Finally, expression of Msi2 was most enriched in the lineage-negative fraction of blast crisis CML (Fig. 2e). These data indicate that Msi2 expression associates predominantly with normal haematopoietic stem cells and the most immature fraction of leukaemic cells.

Because Msi2 and Numb were expressed in a reciprocal pattern, we tested whether Msi2 could repress Numb during leukaemogenesis. Expression of Msi2 in chronic phase CML cells led to downregulation of Numb (Fig. 2f, g). Furthermore, NUP98–HOXA9 could also activate this cascade by increasing expression of Msi2 (Fig. 2h). Because NUP98–HOXA9 initiates transformation through HoxA9-mediated DNA binding and transcription, we tested whether HoxA9 could bind the Msi2 promoter and activate its expression directly. Chromatin immunoprecipitation revealed that HoxA9 was associated with the putative HoxA9-binding element we identified at −5.7 kb (Fig. 2i–l). NUP98–HOXA9 expression was also able to induce Msi2 reporter activity in KLS cells (Fig. 2m and Supplementary Fig. 6a). These data show that Msi2 can be upregulated by NUP98–HOXA9 and subsequently contribute to blast crisis CML by repressing Numb.

To test if Msi2 is required for the development of blast crisis CML, we used a mouse in which the *Msi2* gene was disrupted by a gene-trap (Gt) vector[25] (Supplementary Fig. 6a, b). *Msi2* mutant mice were viable, albeit smaller and less frequent than predicted ($Msi2^{+/+}$:$Msi2^{+/Gt}$:$Msi2^{Gt/Gt}$ = 38:66:19, $P = 0.038$), and showed a two–three-fold reduction in the frequency (Fig. 3a) and absolute number (data not shown) of KLS cells. Additionally, loss of Msi2 led to significantly impaired leukaemia growth *in vivo* (Fig. 3b, 93% for control versus 57% for $Msi2^{Gt/Gt}$).

To determine whether inhibiting Msi2 could have an impact on the growth of established CML, and to rule out the possibility that the reduced incidence of leukaemia in gene-trap mutants was due to developmental defects, Msi expression was targeted using an alternative short hairpin (sh)RNA approach (Supplementary Fig. 7a). Delivery of Msi2 shRNAs (shMsi) into established blast crisis CML cells increased Numb expression (data not shown) and reduced leukaemia growth *in vitro* (Fig. 3c and Supplementary Fig. 7b–e) and *in vivo* (Fig. 3d). Further, the majority of leukaemias that occurred in the presence of shMsi were more differentiated (Fig. 3e) and impaired in their ability to propagate disease (Fig. 3f, 88% control versus 25% shMsi). These data show that Msi2 is important for the establishment and continued propagation of blast crisis CML.

Finally, we examined whether MSI2 was aberrantly upregulated during human leukaemia progression. MSI2 was tracked in 30 patient samples from repositories in Korea and the United Kingdom, and found to be expressed at significantly higher levels in blast crisis

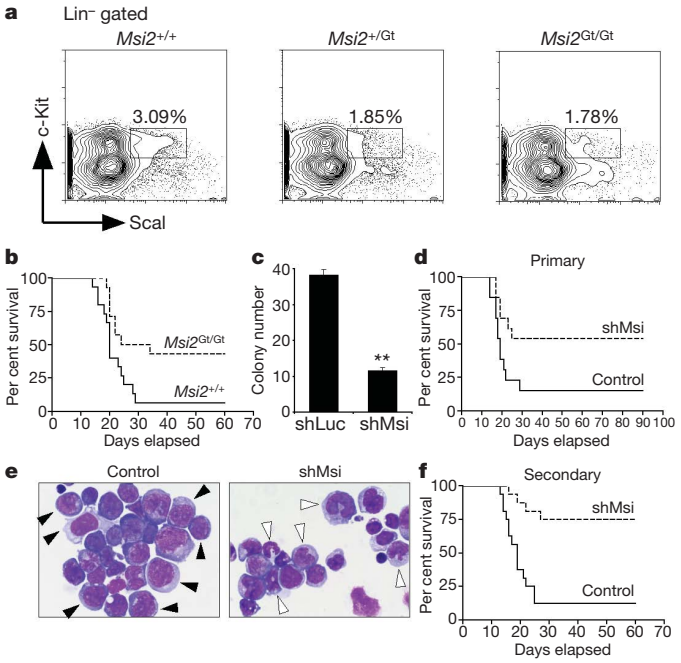

Figure 3 | Loss of Musashi impairs the development and propagation of blast crisis CML **a**, Representative FACS plots showing frequency of KLS cells in mice of the indicated genotypes ($Msi2^{+/+}$, $n = 4$; $Msi2^{+/Gt}$, $n = 3$; $Msi2^{Gt/Gt}$, $n = 4$). **b**, Survival curve of mice transplanted with BCR–ABL- and NUP98–HOXA9-infected $Msi2^{+/+}$ or $Msi2^{Gt/Gt}$ KLS cells ($Msi2^{+/+}$, $n = 15$; $Msi2^{Gt/Gt}$, $n = 14$; $^{*}P = 0.0159$). **c**, Colony-forming ability of blast crisis CML cells transduced with control shRNA (shLuc) or Msi2 shRNA (shMsi). Error bars represent s.e.m. $^{**}P < 0.001$. **d**, Survival curve of mice transplanted with established blast crisis CML cells infected with control shLuc or shMsi ($n = 13$ each; $^{*}P = 0.0267$). **e**, Wright's stain of leukaemic cells from mice transplanted with control shLuc- or shMsi-infected blast crisis CML. Immature myeloblasts, filled arrowheads; differentiating myelocytes and mature band cells, open arrowheads. Original magnification, ×100. **f**, Survival curve of mice transplanted with Lin^{-} cells from primary shRNA-expressing leukaemias ($n = 16$ each; $^{**}P < 0.001$). Data shown is representative of two to three independent experiments.

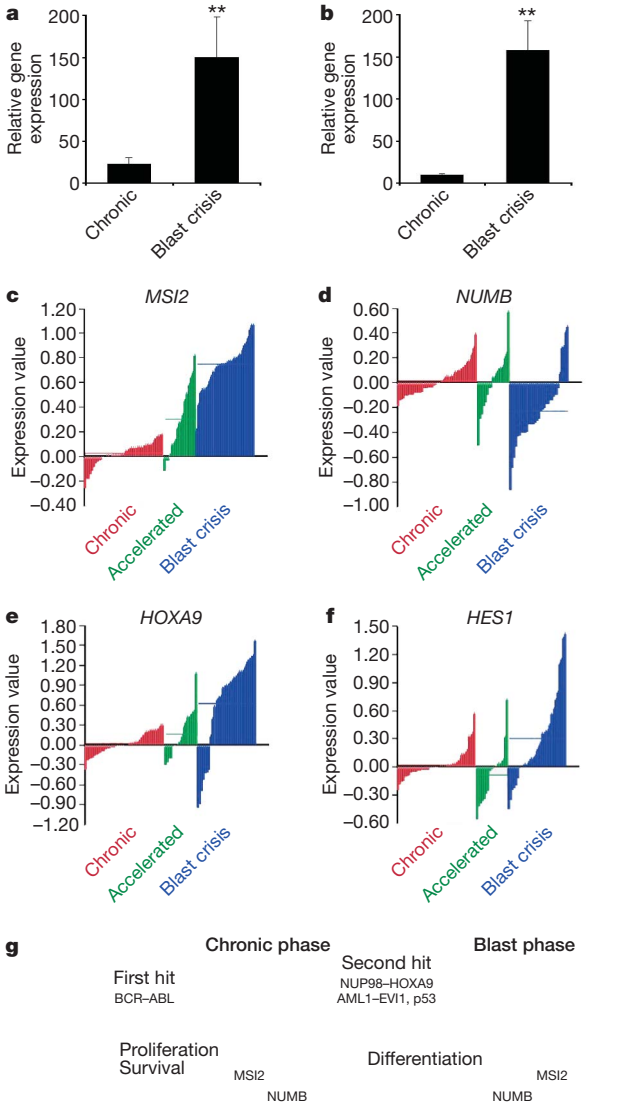

Figure 4 | Musashi expression is upregulated during human CML progression. **a**, **b**, PCR analysis of *MSI2* expression in chronic and blast crisis CML patient samples from the Korean Leukaemia Bank, Korea ($n = 9$ per cohort, Mann–Whitney *U*-test, $^{**}P < 0.001$) (**a**), and the Hammersmith MRD Lab Sample Archive, United Kingdom ($n = 6$ per cohort, Mann–Whitney *U*-test, $^{**}P < 0.001$) (**b**). Error bars represent s.e.m. **c**–**f**, Microarray analysis of expression of *MSI2* (**c**), *NUMB* (**d**), *HOXA9* (**e**) (all $P < 0.001$) and *HES1* (**f**) ($P = 0.68$) in bone marrow and peripheral blood samples from 42 chronic (red), 17 accelerated (green) and 31 blast crisis phase (blue) patients in the United States. **g**, Proposed model for the role of MSI2 and NUMB in CML progression.

CML (Fig. 4a, b). To determine if this reflected a general pattern in human CML progression, we examined the expression of MSI2 and associated genes in 90 patient samples from banks in the United States[26]. Microarray analysis revealed a marked upregulation of MSI2 in every patient during CML progression (Fig. 4c). Furthermore, NUMB was downregulated in a majority of blast crisis patients (Fig. 4d). Notably, our mouse model was driven by NUP98–HOXA9 as a second hit, whereas human blast crisis CML patients harbour a variety of secondary mutations. Because Msi2 could be regulated by HoxA9 expression in the mouse model of CML, we examined whether HOXA9 was upregulated in blast crisis CML samples. The observation that a majority of patient samples had elevated levels of HOXA9 (Fig. 4e) may explain how MSI2 becomes upregulated in advanced stage disease regardless of the nature of the second hit. Notch signalling targets HES1 and TRIB2 were also elevated in a number of blast crisis patient samples (Fig. 4f and Supplementary Fig. 8), consistent with other independent reports[27].

Because the highest MSI2 expression was observed in blast crisis patients, where treatment outcomes are extremely poor, and because a range of expression was observed in both chronic and accelerated phase CML, we tested whether MSI2 expression correlated with outcome after allogeneic transplantation. Patients were divided into two groups based on median expression of MSI2. Among 37 chronic phase patients with available outcomes (9 relapses), increased MSI2 expression was associated with a higher risk of relapse (hazard ratio = 4.35; 95% confidence interval, 0.90–21.06, $P = 0.07$). Additionally, among 13 accelerated phase patients with available outcomes (6 deaths and 3 relapses), increased MSI2 expression was not only associated with higher risk of relapse (all relapses occurred in the increased MSI2 group, $P = 0.06$) but also with higher risk of death (hazard ratio = 6.76; 95% CI, 0.78–58.57, $P = 0.08$). The association of MSI2 with poorer outcomes indicates that MSI2 may be an early marker of advanced CML disease.

Our work identifies the Musashi–Numb axis as an important regulator of myeloid leukaemia and indicates that maintenance of the immature state is dependent on reversal of classical differentiation cues. Specifically, we find that MSI2 is upregulated and NUMB downregulated as chronic phase CML progresses to blast crisis, and that modulation of this pathway can inhibit disease (Fig. 4g). Although previous work has implicated Musashi and Numb in normal development[13,14,23,24], to our knowledge this is the first demonstration that this pathway is required for haematological malignancy.

Our previous work showing that whereas BCR–ABL cannot affect the choice between asymmetric and symmetric division, NUP98–HOXA9 can trigger a bias towards symmetric renewal[15], had led us

to propose that regulators of asymmetric division might regulate leukaemic differentiation, and could thus be targets for therapy in advanced myeloid leukaemia. Our current work supports this and shows that Numb, which drives commitment and differentiation, can impair blast crisis CML establishment and propagation. It should be noted that just as Numb's influence may be mediated through p53 and/or Notch signalling[12,13,20], Musashi may act through Numb as well as other targets such as $p21^{WAF1}$ (refs 21, 28).

Because blast crisis CML is uniformly resistant to current treatments, it is critical to identify new pathways that drive this aggressive disease. In that context, our work is important because it shows that specific differentiation cues associated with the Musashi–Numb cascade can unlock the differentiation potential of blast crisis CML and impair its growth. These data, together with the fact that Musashi seems to be an early marker of advanced CML, indicate that its expression could serve as a prognostic tool, and that targeting it might represent a new approach to therapy. Finally, reports of increased expression of Musashi in glioblastoma[29] and decreased expression of NUMB in high-grade breast cancer[30] raise the possibility that this pathway may also be relevant in solid cancers.

METHODS SUMMARY

Mouse models of CML were generated by transducing bone marrow stem and progenitor cells with retroviruses carrying BCR–ABL (chronic phase) or BCR–ABL and NUP98–HOXA9 (blast crisis phase) and transplanting them into irradiated recipient mice. The development of CML was confirmed by flow cytometry and histopathology. For Msi2 knockdown experiments, lineage-negative blast crisis CML cells were infected with Msi2 or control Luciferase shRNA retroviral constructs and leukaemia incidence monitored. Chromatin immunoprecipitation (ChIP) assays were performed using the myeloid leukaemia cell line M1. DNA was crosslinked and immunoprecipitated with control or anti-HOXA9 antibodies and analysed by PCR for regions of interest. CML patient samples were obtained from the Korean Leukaemia Bank (Korea), the Hammersmith MRD Lab Sample Archive (United Kingdom), the Fred Hutchinson Cancer Research Center (United States) and the Singapore General Hospital (Singapore). Gene expression in human chronic and blast crisis CML was analysed by PCR or by DNA microarrays.

Full Methods and any associated references are available in the online version of the paper at www.nature.com/nature.

Received 7 August 2008; accepted 13 May 2010.
Published online 18 July 2010.

1. Calabretta, B. & Perrotti, D. The biology of CML blast crisis. *Blood* **103,** 4010–4022 (2004).
2. Daley, G. Q., Van Etten, R. A. & Baltimore, D. Induction of chronic myelogenous leukemia in mice by the P210bcr/abl gene of the Philadelphia chromosome. *Science* **247,** 824–830 (1990).
3. Pear, W. S. *et al.* Efficient and rapid induction of a chronic myelogenous leukemia-like myeloproliferative disease in mice receiving P210 bcr/abl-transduced bone marrow. *Blood* **92,** 3780–3792 (1998).
4. Uemura, T., Shepherd, S., Ackerman, L., Jan, L. Y. & Jan, Y. N. *numb*, a gene required in determination of cell fate during sensory organ formation in *Drosophila* embryos. *Cell* **58,** 349–360 (1989).
5. Nakamura, M., Okano, H., Blendy, J. A. & Montell, C. Musashi, a neural RNA-binding protein required for *Drosophila* adult external sensory organ development. *Neuron* **13,** 67–81 (1994).
6. Mayotte, N., Roy, D. C., Yao, J., Kroon, E. & Sauvageau, G. Oncogenic interaction between BCR-ABL and NUP98-HOXA9 demonstrated by the use of an *in vitro* purging culture system. *Blood* **100,** 4177–4184 (2002).
7. Dash, A. B. *et al.* A murine model of CML blast crisis induced by cooperation between BCR/ABL and NUP98/HOXA9. *Proc. Natl Acad. Sci. USA* **99,** 7622–7627 (2002).
8. Witte, O. The role of Bcr-Abl in chronic myeloid leukemia and stem cell biology. *Semin. Hematol.* **38,** 3–8 (2001).
9. Ren, R. Mechanisms of BCR-ABL in the pathogenesis of chronic myelogenous leukaemia. *Nature Rev. Cancer* **5,** 172–183 (2005).
10. Melo, J. V. & Barnes, D. J. Chronic myeloid leukaemia as a model of disease evolution in human cancer. *Nature Rev. Cancer* **7,** 441–453 (2007).
11. Goldman, J. M. & Melo, J. V. BCR-ABL in chronic myelogenous leukemia–how does it work? *Acta Haematol.* **119,** 212–217 (2008).
12. Knoblich, J. A. Mechanisms of asymmetric cell division during animal development. *Curr. Opin. Cell Biol.* **9,** 833–841 (1997).
13. Spana, E. P. & Doe, C. Q. Numb antagonizes Notch signaling to specify sibling neuron cell fates. *Neuron* **17,** 21–26 (1996).
14. Shen, Q., Zhong, W., Jan, Y. N. & Temple, S. Asymmetric Numb distribution is critical for asymmetric cell division of mouse cerebral cortical stem cells and neuroblasts. *Development* **129,** 4843–4853 (2002).
15. Wu, M. *et al.* Imaging hematopoietic precursor division in real time. *Cell Stem Cell* **1,** 541–554 (2007).
16. Wang, H., Ouyang, Y., Somers, W. G., Chia, W. & Lu, B. Polo inhibits progenitor self-renewal and regulates Numb asymmetry by phosphorylating Pon. *Nature* **449,** 96–100 (2007).
17. Neering, S. J. *et al.* Leukemia stem cells in a genetically defined murine model of blast-crisis CML. *Blood* **110,** 2578–2585 (2007).
18. Justice, N., Roegiers, F., Jan, L. Y. & Jan, Y. N. Lethal giant larvae acts together with numb in notch inhibition and cell fate specification in the *Drosophila* adult sensory organ precursor lineage. *Curr. Biol.* **13,** 778–783 (2003).
19. Wakamatsu, Y., Maynard, T. M., Jones, S. U. & Weston, J. A. NUMB localizes in the basal cortex of mitotic avian neuroepithelial cells and modulates neuronal differentiation by binding to NOTCH-1. *Neuron* **23,** 71–81 (1999).
20. Colaluca, I. N. *et al.* NUMB controls p53 tumour suppressor activity. *Nature* **451,** 76–80 (2008).
21. Imai, T. *et al.* The neural RNA-binding protein Musashi1 translationally regulates mammalian numb gene expression by interacting with its mRNA. *Mol. Cell. Biol.* **21,** 3888–3900 (2001).
22. Okabe, M., Imai, T., Kurusu, M., Hiromi, Y. & Okano, H. Translational repression determines a neuronal potential in *Drosophila* asymmetric cell division. *Nature* **411,** 94–98 (2001).
23. Sakakibara, S. *et al.* RNA-binding protein Musashi family: roles for CNS stem cells and a subpopulation of ependymal cells revealed by targeted disruption and antisense ablation. *Proc. Natl Acad. Sci. USA* **99,** 15194–15199 (2002).
24. Okano, H. *et al.* Function of RNA-binding protein Musashi-1 in stem cells. *Exp. Cell Res.* **306,** 349–356 (2005).
25. Taniwaki, T. *et al.* Characterization of an exchangeable gene trap using pU-17 carrying a stop codon-*βgeo* cassette. *Dev. Growth Differ.* **47,** 163–172 (2005).
26. Radich, J. P. *et al.* Gene expression changes associated with progression and response in chronic myeloid leukemia. *Proc. Natl Acad. Sci. USA* **103,** 2794–2799 (2006).
27. Nakahara, F. *et al.* Hes1 immortalizes committed progenitors and plays a role in blast crisis transition in chronic myelogenous leukemia. *Blood* **115,** 2872–2881 (2010).
28. Battelli, C., Nikopoulos, G. N., Mitchell, J. G. & Verdi, J. M. The RNA-binding protein Musashi-1 regulates neural development through the translational repression of $p21^{WAF-1}$. *Mol. Cell. Neurosci.* **31,** 85–96 (2006).
29. Liu, G. *et al.* Analysis of gene expression and chemoresistance of $CD133^{+}$ cancer stem cells in glioblastoma. *Mol. Cancer* **5,** 67 (2006).
30. Pece, S. *et al.* Loss of negative regulation by Numb over Notch is relevant to human breast carcinogenesis. *J. Cell Biol.* **167,** 215–221 (2004).

Supplementary Information is linked to the online version of the paper at www.nature.com/nature.

Acknowledgements We thank A. M. Pendergast, J. Chute, K. Itahana, L. Penalva and L. Grimes for advice and reagents; K.-i. Yamamura for the *Msi2* gene-trap mice; T. Honjo for the Rbpj conditional mice; N. Gaiano for the TNR mice; D. Baltimore for the lentiviral shRNA constructs; and A. Means and B. Hogan for comments on the manuscript. We also thank M. Cook, B. Harvat and L. Martinek for cell sorting; M. Fereshteh for advice on analysis of patient samples; D. McDonnell and H. Wade for advice on ChIP experiments; S. W. Tian for help in collecting patient samples and A. Chen and S. Honeycutt for technical help. The BCR–ABL construct was a gift from W. Pear and the NUP98–HOXA9 construct a gift from G. Gilliland. T.I. is the recipient of a postdoctoral fellowship from the Astellas Foundation for Research on Metabolic Disorders, K.L.C. is the recipient of an American Heart Association predoctoral award, B.Z. received support from T32 GM007184-33 and T.R. is the recipient of a Leukemia and Lymphoma Society Scholar Award. This work was also supported by an LLS Translational Research grant and an ASH Junior Faculty Award to V.G.O., as well as NIH grants CA18029 to J.P.R., CA140371 to V.G.O., CA122206 to C.T.J. and DK63031, DK072234, AI067798, HL097767, DP1OD006430 and an Alexander and Margaret Stewart Fund grant to T.R. We are grateful for the support received from the Lisa Stafford Research Prize.

Author Contributions T.I. and H.Y.K. designed the research, performed the majority of the experiments and helped write the paper. B.Z., K.L.C., J.B., W.E.L. and C.Z. provided experimental data and help; A.L. provided histopathological analysis; C.T.J., G.G., L.F., J.G., H.G., S.-H.K., D.-W.K. and C.C. provided human patient samples and experimental advice; T.I., H.Y.K., G.G. and B.Z. defined gene expression in patient samples by PCR; and V.G.O. and J.P.R. carried out all microarray and patient outcome analyses. T.R. conceived of the project, planned and guided the research, and wrote the paper.

Author Information Reprints and permissions information is available at www.nature.com/reprints. The authors declare no competing financial interests. Readers are welcome to comment on the online version of this article at www.nature.com/nature. Correspondence and requests for materials should be addressed to T.R. (t.reya@duke.edu).

METHODS

Mice. C57BL6/J and BA (C57BL/Ka-Thy1.1) mice were used as transplant donors, and B6-CD45.1 (B6.SJL-*Ptprc*^{a} *Pepc*^{b}/BoyJ) and HZ (C57BL/Ka-Thy1.1-CD45.1) mice were used as transplant recipients. All mice were 8–16 weeks of age. *Msi2* mutant mice, B6;CB-*Msi2*$^{Gt(pU-21T)2Imeg}$, were made and established by gene-trap mutagenesis (CARD, Kumamoto University). Floxed *Rbpj* mice, B6.Cg-*Rbpsuh*^{tm3Kyo}, were from RIKEN BioResource Center (RBRC01071), and crossed with *Vav-cre* transgenic mice[31,32]. Mice were bred and maintained in the animal care facility at Duke University Medical Center. All animal experiments were performed according to protocols approved by the Duke University Institutional Animal Care and Use Committee.

Cell isolation and FACS analysis. Haematopoietic stem cells were sorted from mouse bone marrow essentially as described[31]. c-Kit-positive cells were enriched by staining whole bone marrow with anti-CD117/c-Kit microbeads and isolating positively labelled cells with autoMACS cell separation (Miltenyi Biotec). For lineage analysis peripheral blood cells were obtained by submandibular bleeding and diluted in 0.5 ml of 10 mM EDTA in PBS. 1 ml of 2% dextran was then added to each sample, and red blood cells depleted by sedimentation for 45 min at 37 °C. Red blood cells were lysed using RBC Lysis Buffer (eBioscience) before staining for lineage markers. The following antibodies were used to define the lineage positive cells in leukaemic samples: 145-2C11 (CD3ε), GK1.5 (CD4), 53-6.7 (CD8), RB6-8C5 (Ly-6G/Gr-1), M1/70 (CD11b/Mac-1), TER119 (Ly-76/TER119) and 6B2 (CD45R/B220). Other antibodies used for haematopoietic stem cell sorts included 2B8 (CD117/c-Kit) and D7 (Ly-6A/E/Sca-1). All antibodies were purchased from BD Pharmingen or eBioscience. Analysis and cell sorting were carried out on a FACSVantage SE, FACStar, FACSCanto II, or FACSDiva (all from Becton Dickinson) at the Duke Comprehensive Cancer Center Flow Core Facility, and data were analysed with FlowJo software (Tree Star Inc.).

Retroviral constructs and production. BCR-ABL was cloned into MSCV-IRES-GFP, -YFP or -CFP retroviral vector. NUP98-HOXA9 was cloned into the MSCV-IRES-YFP or -tNGFR vector. *Numb* cDNA (p65 isoform, NCBI accession number BC033459) was cloned into the MSCV-IRES-GFP vector. *Msi2* cDNA (IMAGE clone ID 40045350) was purchased from Open Biosystems, and its protein coding region was cloned into MSCV-IRES-GFP or MSCV-IRES-CFP. Short hairpin RNA (shRNA) constructs were designed and cloned in MSCV/LTRmiR30-PIG (LMP) vector from Open Biosystems according to their instructions. The target sequences are 5′-CCCAGATAGCCTTAGAGACTAT-3′ for *Msi2* and 5′-CTGTGCCAGAGTCCTTCGATAG-3′ for firefly luciferase as a negative control. MSCV-IRES-CFP with *Msi2* mutant cDNA resistant to shMsi was constructed by inverse PCR strategy using primers with silent mutations (underlined) in the shMsi target sequence: 5′-CCTGACTCTCTGA GGGACTATTTTAGCAAATTTGG-3′. Lentiviral shRNA construct with the alternative *Msi2* target sequence, 5′-AGTTAGATTCCAAGACGA-3′, was cloned in FG12 as described previously[33]. Virus was produced in 293T cells transfected with viral constructs along with gag-pol, VSV-G and Rev (in case of FG12) constructs. Viral supernatants were collected for 3–5 days and concentrated by ultracentrifugal at 50,000*g* for 3 h.

***In vitro* methylcellulose colony formation assays.** Lineage negative (Lin^{-}), NUP98-HOXA9-IRES-YFP positive cells from blast crisis CML were sorted and infected retrovirally with either Vector-IRES-GFP or Numb-IRES-GFP. After 48 h of infection, cells were sorted and serially plated in complete methylcellulose medium (Methocult GF M3434 from StemCell Technologies). For knockdown experiments, Lin^{-} population in blast crisis CML were sorted and infected with the indicated retroviruses for 48 h. Infected cells were sorted based on their fluorescent protein expression and plated as above. Colonies were counted 5–7 days after plating.

Generation and analysis of leukaemic mice. Bone marrow c-Kit^{+} or KLS cells were sorted and cultured overnight in X-Vivo15 media (BioWhittaker) supplemented with 50 μM 2-mercaptoethanol, 10% fetal bovine serum, stem cell factor (SCF, 100 ng ml^{-1}, R&D Systems) and thrombopoietin (TPO, 20 ng ml^{-1}, R&D Systems). Subsequently, cells were infected with the retroviruses. Viruses used were as follows: MSCV-BCR-ABL-IRES-YFP (or CFP or GFP) to generate chronic phase leukaemia, or MSCV-BCR-ABL-IRES-YFP (or CFP or GFP) and MSCV-NUP98-HOXA9-IRES-tNGFR (or YFP) to generate blast crisis CML. Cells were harvested 48 h after infection and transplanted retro-orbitally into groups of B6-CD45.1 mice. Recipients were lethally irradiated (10 Gy) for chronic phase leukaemia, and sublethally (7 Gy) or non-irradiated for blast crisis CML. For Numb overexpression, cells were infected with either MSCV-Numb-IRES-GFP or MSCV-IRES-GFP along with MSCV-BCR-ABL-IRES-YFP (or CFP) and MSCV-NUP98-HOXA9-IRES-tNGFR (or YFP) and 20,000 to 100,000 infected cells were transplanted per mouse. For secondary transplantation, cells from primary transplanted mice were sorted for either MSCV-Numb-IRES-GFP and MSCV-NUP98-HOXA9-IRES-YFP or MSCV-IRES-GFP and MSCV-NUP98-HOXA9-IRES-YFP, and 7,000 to 8,000 cells were transplanted per mouse. For *Msi2* knockdown by retroviral shRNA transduction, the Lin^{-} population from blast crisis CML were sorted and infected with either control shLuc (against luciferase) or shMsi (against Msi2) retrovirus for 48 h. Infected cells were sorted based on their GFP expression, and 1,000 to 3,000 cells were transplanted in sublethally irradiated B6-CD45.1 recipients. After transplantation, recipient mice were maintained on antibiotic water (sulphamethoxazole and trimethoprim) and evaluated daily for signs of morbidity, weight loss, failure to groom and splenomegaly. Premorbid animals were killed and relevant tissues were harvested and analysed by flow cytometry and histopathology.

Immunofluorescence staining. For immunofluorescence, relevant leukaemic cell populations were sorted, cytospun and fixed in 4% paraformaldehyde for 5 min. Samples were then blocked using 20% normal donkey serum in PBS with 0.1% Tween 20, and stained at 4 °C overnight with an antibody followed by Alexafluor-conjugated secondary antibody (Molecular probe) and DAPI. Slides were mounted using mounting media (Fluoromount-G SouthernBiotech) and viewed on the Axio Imager (Zeiss). Antibodies used were as follows: anti-Numb, Ab4147 (Abcam) or C29G11 (Cell Signaling Technology); anti-p53, DO-1 (Thermo Scientific); anti-cleaved Notch1, Val 1744 (Cell Signaling). Fluorescence intensity was analysed using Metamorph software (Molecular Devices).

ChIP assays. To identify potential HOX binding sites in the *Msi2* gene upstream promoter region, we used an algorithm ConCise Scanner[34] using a combination of the following matrices: V$HOXA9.01, V$HOXB9.01, V$PBX_HOXA9.01, V$HOX_PBX.01, V$MEIS1A_HOXA9.01 and V$MEIS1B_HOXA9.01. The myeloid leukaemia cell line M1 was maintained in RPMI1640 media supplemented with 10% fetal bovine serum, and 1×10^{7} cells were subjected to DNA–protein cross-linking. ChIP assays were performed according to a modified protocol based on the ChIP-IT Express kit (Active Motif). PCR primer sequences are as follows; for *Msi2* (−5.7 kb site), 5′- TGGACAGCCTCATCCACAGAGCA-3′ and 5′-ACTGTGCTACATTCCCAGCCGCT-3′; for *Msi2* (+110 kb site), 5′-GT TCTTAGCTGCCTCTCTCAGA-3′ and 5′-GAACAATGTCTCTGTCAGGC CT-3′; for *Flt3*, 5′-AGTCAGAAGGGACTGGCTCC-3′ and 5′-GAGTGCTG CTTAGCAGATTACC-3′.

β-Galactosidase reporter gene assays. KLS cells were isolated from *Msi2* gene-trap heterozygote bone marrow and infected with MSCV-BCR-ABL-IRES-YFP and MSCV-NUP98-HOXA9-IRES-GFP. GFP and YFP double positive cells were sorted 48 h after infection, and cultured in X-Vivo15 media supplemented with SCF and TPO as described. After 4 days, cells were harvested in reporter lysis reagent, and β-galactosidase activities were analysed by using β-Gal reporter gene assay, Chemiluminescent (Roche Diagnostics).

Real-time and standard RT–PCR analysis. RNA was isolated using RNAqueous-Micro (Ambion), equal amounts of RNAs were converted to cDNA using Superscript II reverse transcriptase (Invitrogen). Quantitative real-time PCRs were performed using an iCycler (BioRad) by mixing cDNAs, iQ SYBRGreen Supermix (BioRad) and gene-specific primers. Results were normalized to the level of β2 microglobulin (*B2m*, mouse) or β-actin (*ACTB*, human). Primer sequences are as follows: *Numb*-F, 5′-ATGAGTTGCCTTCCACTATGCAG-3′; *Numb*-R, 5′-TGCTGAAGGCACTGGTGATCTGG-3′; *Msi1*-F, 5′-ATGGATGCCTTCATGCT GGGT-3′; *Msi1*-R, 5′-CTCCGCTCTACACGGAATTCG-3′; *Msi2*-F, 5′-TGCCA TACACCATGGATGCGT-3′; *Msi2*-R, 5′-GTAGCCTCTGCCATAGGTTGC-3′; *B2m*-F, 5′-ACCGGCCTGTATGCTATCCAGAA-3′; *B2m*-R, 5′-AATGTGAGGCG GGTGGAACTGT-3′; *MSI2*-F, 5′-GTTATCTGCGAACACAGTAGTG-3′; *MSI2*-R, 5′-ACCCTCTGTGCCTGTTGGTAG-3′; *ACTB*-F, 5′-AAGCCACCCCACTTC TCTCTAA-3′; *ACTB*-R, 5′-AATGCTATCACCTCCCCTGTGT-3′. Human *HES1* (Hs00172878_m1) and *TRIB2* (Hs00222224_m1) gene levels were analysed with TaqMan Gene Expression Assays.

Human leukaemia specimens and microarray gene expression studies. Chronic and blast crisis CML samples were obtained from the Korean Leukaemia Bank (Korea), the Hammersmith MRD Lab Sample Archive (UK), the Fred Hutchinson Cancer Research Center (USA) and the Singapore General Hospital (Singapore) from Institutional Review Board approved protocols with written informed consent in accordance with the Declaration of Helsinki. Gene expression profiles of CML patient samples have been described previously[35]. This published data set has been reanalysed to examine expression of *MSI2*, *NUMB*, *HES1* and *HOXA9* in bone marrow and peripheral blood samples from 42 chronic phase, 17 accelerated phase and 31 blast crisis CML patients. The procedures for RNA extraction, amplification, labelling and hybridization, as well as statistical analysis methods for the Rosetta platform, are as previously published[35]. GenePlus software (Enodar Biologic) was used to determine differential expression between groups (that is, by disease phase); *P*-values were calculated using gene-by-gene ANOVA and estimating equation techniques were used to calculate the number of false discoveries[36].

Statistical analysis. The statistical analysis was carried out using the R language version 2.6.2 (http://www.r-project.org/) and GraphPad Prism software version 4.0c (GraphPad software Inc.).

31. Zhao, C. *et al.* Loss of β-catenin impairs the renewal of normal and CML stem cells *in vivo*. *Cancer Cell* **12,** 528–541 (2007).
32. Han, H. *et al.* Inducible gene knockout of transcription factor recombination signal binding protein-J reveals its essential role in T versus B lineage decision. *Int. Immunol.* **14,** 637–645 (2002).
33. Qin, X. F., An, D. S., Chen, I. S. & Baltimore, D. Inhibiting HIV-1 infection in human T cells by lentiviral-mediated delivery of small interfering RNA against CCR5. *Proc. Natl Acad. Sci. USA* **100,** 183–188 (2003).
34. Jegga, A. G. *et al.* Detection and visualization of compositionally similar cis-regulatory element clusters in orthologous and coordinately controlled genes. *Genome Res.* **12,** 1408–1417 (2002).
35. Radich, J. P. *et al.* Gene expression changes associated with progression and response in chronic myeloid leukemia. *Proc. Natl Acad. Sci. USA* **103,** 2794–2799 (2006).
36. Zhao, L. P., Prentice, R. & Breeden, L. Statistical modeling of large microarray data sets to identify stimulus-response profiles. *Proc. Natl Acad. Sci. USA* **98,** 5631–5636 (2001).